Inorg. Chem. **2007**, *46*, 4220–4229

Modification of Spin Crossover Behavior through Solvent Assisted Formation and Solvent Inclusion in a Triply Interpenetrating Three-Dimensional Network

Matthias Bartel,[†] Alina Absmeier,[†] Guy N. L. Jameson,*[,‡] Franz Werner,[§] Kenichi Kato,[#] Masaki Takata,[#] Roman Boca,[||] Miki Hasegawa,[⊥] Kurt Mereiter,[§] Andrea Caneschi,[▽] and Wolfgang Linert*[,†]

Institute of Applied Synthetic Chemistry, Vienna University of Technology, Getreidemarkt 9/163-AC, A-1060 Vienna, Austria, Department of Chemistry, University of Otago, P.O. Box 56, Dunedin, New Zealand, Institute of Chemical Technologies and Analytics, Vienna University of Technology, Getreidemarkt 9/164-SC, A-1060 Vienna, Austria, RIKEN-JASRI/SPring-8, 1-1-1 Kouto, Sayo-gun, Hyogo 679-5198, Japan, CREST, JST, Japan, Institute of Inorganic Chemistry, Slovak Technical University, SK-812 37 Bratislava, Slovakia, College of Science and Engineering, Aoyama-Gakuin University, Sagamihara, Kanagawa 229-8558, Japan, and LAMM, Dipartimento di Chimica & UdR INSTM, Università di Firenze, Via della Lastruccia 3, I-50019 Sesto F.no, Italy

Received January 30, 2007

The 3D coordination polymer $[Fe(4ditz)_3](PF_6)_2 \cdot$solv consists of three interpenetrating infinite networks. There are cavities between iron atoms of different networks, which are partly filled with solvent molecules. With a change of the solvent used during synthesis from methanol to ethanol, the magnetic behavior of the materials changes. Both show an abrupt two-step spin crossover from low spin ($S = 0$) to high spin ($S = 2$) with the methanolate curve lying 7 K higher and showing a small hysteresis. Single crystal and powder diffraction studies show that they both have the same structure, but in powder form, the methanolate slowly loses methanol to finally leave about 0.075 MeOH/Fe. In comparison, the bigger ethanol remains at 0.25 EtOH/Fe. These results, in conjunction with thermodynamic data, strongly suggest that the differences in magnetic behavior are largely entropic in nature. Possible reasons for this are discussed.

Introduction

Coordination polymers are a very productive field of study with interest driven by the hope of forming new materials[1,2] that can be used in many applications such as data storage and seeking an understanding of what causes different structures to be formed.[3] Of particular interest are those coordination polymers forming 3D networks because one could well expect strong cooperative effects between metal centers. This cooperativeness can be made visible when the metal centers exhibit a spin transition or spin crossover (SC).[4] A requirement to build such networks is bridging ligands between metal centers, but to show cooperativity the ligands must be either short to minimize metal−metal distances[5] or conjugated.[6,7] Longer bridging ligands are expected to significantly separate the SC centers and thus be counterproductive. A particularly elegant way to solve this problem

* To whom correspondence should be addressed. E-mail: gjameson@chemistry.otago.ac.nz (G.N.L.J.), wlinert@mail.zserv.tuwien.ac.at (W.L.).
[†] Institute of Applied Synthetic Chemistry, Vienna University of Technology.
[‡] University of Otago.
[§] Institute of Chemical Technologies and Analytics, Vienna University of Technology.
[#] RIKEN-JASRI/SPring-8 and CREST, JST.
[||] Slovak Technical University.
[⊥] Aoyama-Gaukin University.
[▽] Università di Firenze.

(1) Janiak, C. *J. Chem. Soc., Dalton Trans.* **2003**, *14*, 2781−2804.
(2) Gaspar, A. B.; Ksenofontov, V.; Seredyuk, M.; Guetlich, P. *Coord. Chem. Rev.* **2005**, *249* (23), 2661−2676.
(3) Moulton, B.; Zawarotko, M. J. *Chem. Rev.* **2002**, *101*, 1629−1658.
(4) Real, J. A.; Gaspar, A. B.; Munoz, M. C. *J. Chem. Soc., Dalton Trans.* **2005**, *12*, 2062−2079.
(5) Garcia, Y.; Kahn, O.; Rabardel, L.; Chansou, B.; Salmon, L.; Touchagues, J. P. *Inorg. Chem.* **1999**, *38*, 4663−4670.
(6) Niel, V.; Martinez-Augudo, J. M.; Munoz, M. C.; Gaspar, A. B.; Real, J. A. *Inorg. Chem.* **2001**, *40*, 3838−3839.
(7) Niel, V.; Thompson, A. L.; Goeta, A. E.; Enachescu, C.; Hauser, A.; Galet, A.; Munoz, M. C.; Real, J. A. *Chem.—Eur. J.* **2005**, *11*, 2047−2060.

10.1021/ic070173q CCC: $37.00
Published on Web 04/19/2007

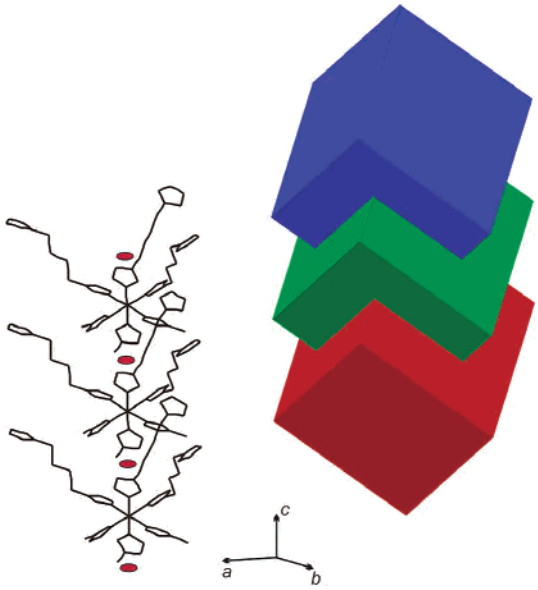

Figure 1. Crystal structure and schematic picture of the 3D network produced by $[Fe(4ditz)_3(PF_6)_2]$·solv. The disordered solvent (red ovals) is statistically distributed in cavities formed between iron atoms of different interpenetrating networks.

is to produce interpenetrating networks,[8,9] which bring the centers closer together, but such structures depend upon many factors including, in some cases, the comparative size of the noncoordinating anion. Within our systematic study of iron(II) SC coordination polymers produced with ditetrazole ligands where the tetrazole moieties are separated by *n*-alkylene spacers of different lengths,[10] we have found that four carbon atoms have exactly the correct length when PF_6^- is used as the noncoordinating anion to produce three 3D networks, which interpenetrate each other (see Figure 1). Between each of these three networks where two iron atoms from different networks face each other, a cavity is produced that is bounded by three tetrazole groups from each octahedrally coordinated iron. Within these cavities solvent molecules are found,[8] which are believed to play a crucial role in the formation of this interpenetrating structure.

Encouraged by this, we have now completed detailed investigations of this system using methanol and ethanol as solvents in order to understand their effect on structure and magnetic behavior. These solvents were chosen because of their chemical and geometrical similarity and because we wanted to keep chemical and ligand-field influences to a minimum. Any large differences will almost certainly affect the energetics of SC or even disrupt the structure and thus make comparison impossible. It is important to note that a similar investigation into the mononuclear complex[11] $[Fe(2\text{-pic})_3]Cl_2$·solv showed a large effect in the magnetic properties by changing the solvent. This complex, however, forms a 2D layer structure through anion−solvent hydrogen bonds and van der Waals interactions between layers. It is probably mainly through this hydrogen-bonded network that the magnetic behavior is changed, although volume or structural changes also play a role. In our system, the solvent is not hydrogen-bonded and, therefore, we hoped to observe either a volume, pressure, or entropy effect, and this is the raison d'être of this paper.

Experimental Section

Chemicals and Standard Physical Characterization. Tetrabutylammonium hexafluorophosphate (98%), iron powder (p.a.), and all other reagents were standard reagent grade and used as supplied. Iron(II)chloride tetrahydrate was freshly prepared from iron powder and aqueous HCl. Elemental analyses (C, H, and N) were performed by the Mikroanalytisches Laboratorium, Faculty of Chemistry, Vienna University, Währingerstrasse 42, A-1090 Vienna, Austria. Midrange FTIR spectra of the compounds were recorded as KBr-pellets within the range of 4400−450 cm^{-1} using a Perkin-Elmer 16PC FTIR spectrometer. Pellets were obtained by pressing the powdered mixture of the samples in KBr in vacuo using a hydraulic press applying a pressure of 10 000 kg cm^{-2} for 5 min. NMR spectra were recorded on a Bruker DPX 200 MHz spectrometer. ^1H NMR chemical shifts are reported in ppm calibrated to the respective solvent.

Synthesis of the Complexes. [*μ*-Tris-(1,4-bis(tetrazol-1-yl)-butane-*N*4,*N*4′)iron(II)]-bis(hexafluorophosphate) Solvate ($[Fe(4ditz)_3](PF_6)_2$·solv). The synthesis of the ligand has been reported[12] in the literature. The syntheses of the complexes were performed under inert gas atmosphere, and only absolute ethanol or methanol was used. Independent of the solvent, the procedure for the synthesis of the two compounds was the same. ***Warning!*** *Tetrazole compounds should be handled with care; they may detonate upon heating or shock.*

1,4-Bis(tetrazole-1-yl)butane (2.6 mmol, 0.5 g) was dissolved in 60 mL of the respective hot solvent. After the solution cooled down to 55 °C, iron(II)chloride tetrahydrate (0.9 mmol, 0.179 g) was added to the solution. Afterward, tetrabutylammonium-hexafluorophosphate (1.7 mmol, 0.659 g) was dissolved in the required solvent and added slowly to the solution. The obtained mixture was stirred for 1 h at room temp. The precipitate was filtered off and stored under argon atmosphere.

$[Fe(4ditz)_3](PF_6)_2$·*x*MeOH (20%, 0.165 g). Elemental analysis calculated[13] for $x = 0.075$, i.e., $C_{18}H_{30}F_{12}FeN_{24}P_2$·0.075MeOH: C 23.5, H 3.4, N 35.66%. Found: C 23.4, H 3.15, N 35.93%. Selected mid-FTIR bands: 3166 cm^{-1} (ν_{C1-H1} of the aromatic tetrazole ring), 2986, 2964, 2941, and 2878 cm^{-1} (ν_{C-H} of the aliphatic C−H in the butylene spacer) (see also Supporting Information, p S1).

$[Fe(4ditz)_3](PF_6)_2$·0.25EtOH (25%, 0.211 g). Elemental analysis calculated for $C_{18}H_{30}F_{12}FeN_{24}P_2$·0.25EtOH: C 23.80, H 3.48, N 35.35%. Found: C 23.58, H 3.18, N 35.76%. Selected mid-FTIR bands: 3167 cm^{-1} (ν_{C1-H1} of the aromatic tetrazole ring), 2990, 2964, 2942, and 2879 cm^{-1} (ν_{C-H} of the aliphatic C−H in the butylene spacer) (see also Supporting Information, p S1).

Single crystals of the complexes were obtained by H-tube slow diffusion. A total of 0.43 mmol of tetrabutylammonium-hexafluo-

(8) Grunert, C. M.; Schweifer, J.; Weinberger, P.; Linert, W.; Mereiter, K.; Hilscher, G.; Mueller, M.; Wiesinger, G.; van Koningsbruggen, P. J. *Inorg. Chem.* **2004**, *43*, 155−165.
(9) Galet, A.; Niel, V.; Munoz, M. C.; Real, J. A. *J. Am. Chem. Soc.* **2003**, *125*, 14224−14225.
(10) Absmeier, A.; Bartel, M.; Carbonera, C.; Jameson, G. N. L.; Weinberger, P.; Caneschi, A.; Mereiter, K.; Letard, J.-F.; Linert, W. *Chem.—Eur. J.* **2006**, *12*, 2235−2243.
(11) Hostettler, M.; Toernroos, K. W.; Chernyshov, D.; Vangdal, B.; Buergi, H.-B. *Angew. Chem., Int. Ed.* **2004**, *43*, 4589−4594.
(12) van Koningsbruggen, P. J.; Garcia, Y.; Koojiman, H.; Spek, A. L.; Haasnoot, J. G.; Kahn, O.; Linares, J.; Codjovi, E.; Varret, F. *J. Chem. Soc., Dalton Trans.* **2001**, *4*, 466−471.
(13) Methanol is slowly lost over time, finally reaching a value of 0.075 as is discussed later.

rophosphate was dissolved in 10−15 mL of hot solvent and placed in one side of the H-tube. On the other side of the tube, 10−15 mL of a hot methanolic or ethanolic solution containing 0.65 mmol of 1,4-bis(tetrazole-1-yl)butane and 0.23 mmol of iron(II)chloride tetrahydrate was added. The colorless single crystals of the complexes were obtained after 1 day (ethanol) or 4 days (methanol).

Magnetic Susceptibility. Magnetic measurements were completed on a SQUID Cryogenix S600 magnetometer with an applied field of 1 T within the temperature range of 140−200 K in the settle mode at atmospheric pressure. All measurements were performed on polycrystalline powder samples weighing ∼10 mg. The data were corrected for the magnetization of the sample holder (Teflon capsule, correction independently determined) and for diamagnetic contributions, calculated with Pascal's constants (see Supporting Information, p S2).

Crystallographic Studies. Four crystals of $[Fe(4ditz)_3](PF_6)_2$·solv, two grown from methanol and two grown from ethanol, were measured on a Bruker SMART CCD three-axis diffractometer using graphite-monochromated Mo Kα radiation from a sealed X-ray tube ($\lambda = 0.710\ 73$ Å) and a Bruker Kryoflex gas stream cooling device. After raw data extraction with the program SAINT, absorption and related effects were corrected with the program SADABS,[14] and data reduction was carried out with the program XPREP. The structures were refined on F^2 with the program SHELX97,[15] paying particular attention to the disordered solvents. Further details of this study are outlined in the supporting material (pp S3−S8 and CIF file).

Synchrotron Powder Diffraction Studies. For precise determination of the lattice parameters, a synchrotron radiation powder diffraction experiment was carried out by using the large Debye−Scherrer camera installed at the BL02B2 beamline, SPring-8 (Sayogun, Japan), that is equipped with an imaging plate detector.[16] With this camera, both high-angular resolution and high-counting statistics data can be collected. The as-precipitated phases were sealed in 0.3 mm glass capillaries. The X-ray powder patterns were measured from 300 K down to 9 K. (A He gas circulation type cryostat was used for the low-temperature measurements.) All data were collected under the same experimental conditions except for the temperature. The exposure time of X-rays was 5 min for each temperature. The wavelength of the incident X-rays was approximately 1 Å. The exact value was determined from a CeO_2 standard. The patterns were recorded with a step width of 0.01° in 2θ in the range $2\theta = 0-75°$, which corresponds to a resolution of $d = 0.82$ Å. The lattice parameters were determined from the powder diffraction patterns by Le Bail extraction[17] using the program GSAS.[18] The reflection profiles were modeled with a pseudo-Voigt function, extended with Stephens' approach of anisotropic microstrain broadening[19] as implemented with profile function no. 4 in the GSAS code. Details on the course of the Le Bail refinements and a table with the so obtained lattice parameters are given in the Supporting Information pp S9−S11.

DSC Calorimetry. A DSC-60 apparatus (Shimadzu) was used to record the heat flow of the samples (2.30 mg) using a free sample holder (aluminum pan) and the sapphire filled container (scan rate, 10 °C/min). The data were analyzed as reported previously.[20]

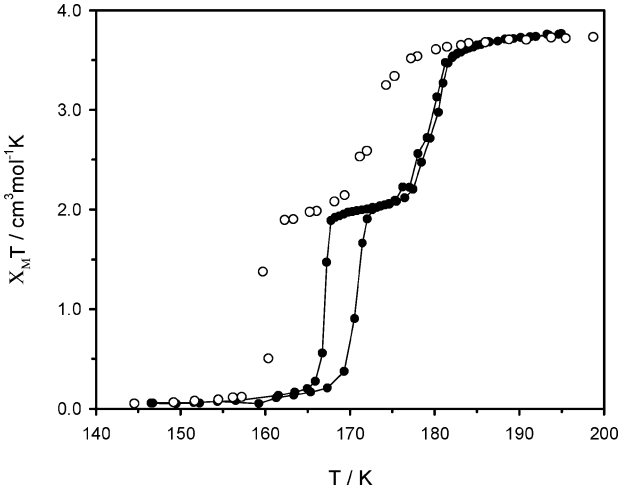

Figure 2. Variable temperature magnetic susceptibility curves ($\chi_M T$ vs T) for (●) $[Fe(4ditz)_3](PF_6)_2$·0.075MeOH and (○) $[Fe(4ditz)_3](PF_6)_2$·0.25EtOH.

Results

Magnetic Measurements. Susceptibility curves were recorded between 140 and 200 K for both samples, $[Fe(4ditz)_3](PF_6)_2$·0.075MeOH and $[Fe(4ditz)_3](PF_6)_2$·0.25EtOH. Figure 2 shows the obtained $\chi_M T$ versus T curves, where χ_M is the molar magnetic susceptibility and T is the temperature. The curve corresponding to $[Fe(4ditz)_3](PF_6)_2$·0.075MeOH is identical to that previously published[8] and shows a steep two-step transition from $S = 0$ to $S = 2$ with a plateau between 168 and 176 K. Furthermore, the first half of the transition at lower temperature shows a hysteresis of approximately 4 K. Compared with this, the $[Fe(4ditz)_3](PF_6)_2$·0.25EtOH curve differs in two ways: the ethanolate is shifted 7 K lower in temperature and does not show hysteresis.

Crystal Structure. The crystal structure of the compound synthesized in methanol has been presented earlier.[8] In this previous work, however, a small amount of chloroform was added to aid crystallization. This has since been found not to be necessary, although crystallization then takes significantly longer. The structure of these new methanolate crystals has been compared with the previous structure and shown to be identical within the limits of error, including the electron density in the solvent cavities (see below), showing that chloroform is not included. In the case of ethanol, the solubility of the ligand and more importantly the complex is significantly lower. Thus, the complex precipitates out of solution too quickly, hindering the formation of larger crystals. This problem was solved by lowering the concentrations slightly, but even then crystallization occurred faster than from methanol and was difficult to control.

The structure of the ethanolate is seen to be identical to the methanolate (see Table 1). There is, however, normal

(14) Bruker programs: *SMART*, version 5.629; *SAINT*, version 6.54; *SADABS* version 2.10; *XPREP*, version 6.14; *SHELXTL*, version 6.14; Bruker AXS Inc.: Madison, WI, 2003.
(15) Sheldrick, G. M. *SHELX97: Program System for Crystal Structure Determination*; University of Göttingen: Göttingen, Germany, 1997.
(16) Takata, M.; Nishibori, E.; Kato, K.; Kubota, Y.; Kuroiwa, Y.; Sakata, M. *Adv. X-Ray Anal.* **2002**, *45*, 377−384.
(17) Le Bail, A.; Duroy, H.; Fourquet, J. L. *Mater. Res. Bull.* **1988**, *23*, 447−452.
(18) Larson, A. C.; Von Dreele, R. B. *General Structure Analysis System (GSAS)*; Los Alamos National Laboratory Report LAUR 86-748; Los Alamos National Laboratory: Los Alamos, NM, 2004; pp 86−748.
(19) Stephens, P. W. *J. Appl. Crystallogr.* **1999**, *32*, 281−289.
(20) Boca, R.; Boca, M.; Dlhan, L.; Falk, K.; Fuess, H.; Haase, W.; Jarosciak, R.; Papankova, B.; Renz, F.; Vrbova, M.; Werner, R. *Inorg. Chem.* **2001**, *40*, 3025−3033.

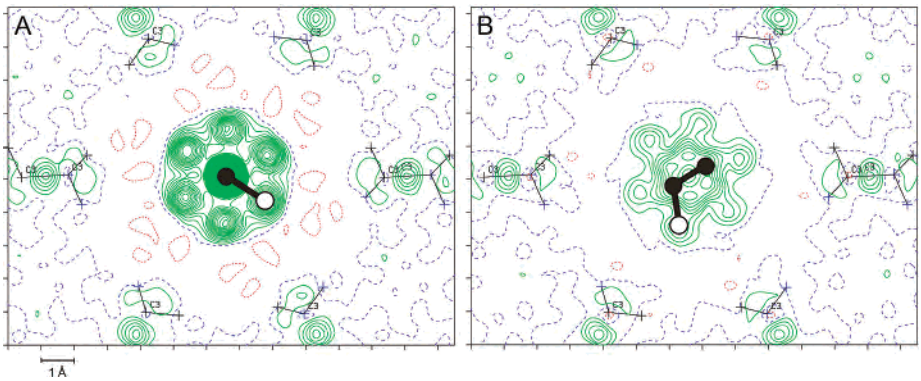

Figure 3. Contoured solvent difference Fourier synthesis parallel to (001) centered at $x,y,z = 0,0,^1/_2$ (SG $P\bar{3}$, Wyckoff position 1b, point symmetry C_{3i}): (A) for methanolate and (B) for ethanolate. The dotted lines refer to 0 e Å^{-3} and increase in steps of 0.25 e Å^{-3} for methanolate (A) and 0.10 e Å^{-3} for ethanolate (B). Logical orientations of the respective solvent have been overlaid for clarity. The peripheral difference density peaks between pairs of C3 atoms are due to C−C bond electrons.

Table 1. Selected Crystallographic Data for $[Fe(4ditz)_3](PF_6)_2 \cdot$solv at 100 K[a]

sample designation	1130 methanol solvate	1124 methanol solvate	1102 ethanol solvate	1098 ethanol solvate
formula	$[Fe(4ditz)_3](PF_6)_2 \cdot 0.75(CH_3OH)$	$[Fe(4ditz)_3](PF_6)_2 \cdot 0.75(CH_3OH)$	$[Fe(4ditz)_3](PF_6)_2 \cdot 0.25(C_2H_5OH)$	$[Fe(4ditz)_3](PF_6)_2 \cdot 0.25(C_2H_5OH)$
formula weight	952.48	952.48	939.97	939.97
a/Å	10.9686(3)	10.963(2)	10.9726(4)	10.9697(5)
c/Å	8.6941(5)	8.6978(16)	8.6916(7)	8.6824(8)
V/Å^3	905.85(6)	905.4(3)	906.25(9)	904.81(10)
ρ_{calcd}/g cm^{-3}	1.746	1.747	1.722	1.725
R1 all/$I > 2\sigma(I)$	0.0216/0.0215	0.0332/0.0307	0.0334/0.0293	0.0372/0.0333
wR2 all/$I > 2\sigma(I)$	0.0553/0.0552	0.0798/0.0783	0.0766/0.0729	0.0803/0.0780
GOF	1.059	1.056	1.054	1.052

[a] For all structures: crystal system trigonal, space group $P\bar{3}$ (No. 147), $Z = 1$, colorless at 300 K, violet at 100 K. The solvent content of the four crystals are slightly idealized but correspond well with the results of the structure refinement.

variation between crystals of the same solvent. Synchrotron data were therefore used to more accurately and reliably determine the cell parameters, allowing any small differences to be compared (see below). The only difference between the two structures is the electron density present in the cavities between iron atoms of different networks and represents less than unit quantities of solvent distributed statistically within the crystal. The difference between solvents can be clearly seen in Figure 3, where a difference Fourier synthesis has been used to plot contour maps parallel to the 001 plane at $z = 0.5$. This shows that the solvent lies perpendicular to the *c*-axis between two iron atoms (see also Figure 1). In both cases the dotted line refers to 0 e Å^{-3} (electrons per cubic angstrom) and increases in steps of 0.25 e Å^{-3} for methanol (Figure 3A) and 0.10 e Å^{-3} for ethanol (Figure 3B). Thus, the electron density is far higher in the case of methanol than in ethanol, and this suggests higher concentrations of methanol than ethanol within the crystals.

The shape of this electron density gives important information about the solvent present, and a model to explain the data can be suggested because the electron density of carbon and oxygen can be identified. In the case of methanol, the CH_3 group lies in the center while the OH group lies in one of six positions defined by the symmetry of the crystal, which includes a C_{3i} operation. For this reason the density of the central carbon is approximately 6 times that of the outer oxygens (compare 6.8 e Å^{-3} with 1.0 e Å^{-3}). This density corresponds to approximately 0.75 methanol molecules per iron. In support of this model, the CO distance is the value expected for methanol (1.41 Å). For clarity, a methanol molecule is drawn in one of the six possible positions in Figure 3A. The geometry shows that any OH interaction with the tetrazoles will occur via the π electrons approximately 1.5 Å away if one takes into account a 1.0 Å OH bond length and a bond angle of approximately 115°. Such interactions have previously been proposed.[21]

The ethanolate can be considered in the same way. In this case the CH_3 and CH_2 groups are not separately identifiable as they lie on top of each other as the molecule takes one of six possible orientations. The OH group does not lie on the same plane as the carbon atoms but lies either above or below as defined by the C_{3i} operation (3D pictures are given in Figure 9 and the Supporting Information, p S8). Three possible positions of the O atoms have, therefore, a higher density in the contour map given in Figure 3B where a representative ethanol molecule has been added. The OH groups are thus closer to the tetrazole π density than if they were inplane, and this adds weight to the suggestion that there is an interaction between these groups. The lower overall electron density present corresponds to 0.25 ethanol molecules per iron.

Synchrotron Powder Diffraction. The results of a typical Le Bail extraction are given in Figure 4. The low agreement indices, together with the small standard deviations of the fitted parameters (see Supporting Information, p S10),

(21) Zhang, R. B.; Somers, R. F.; Kryachko, E. S.; Nguyen, M. T.; Zeegers-Huyskens, T.; Ceulemans, A. *J. Phys. Chem. A* **2005**, *109*, 8028−8034.

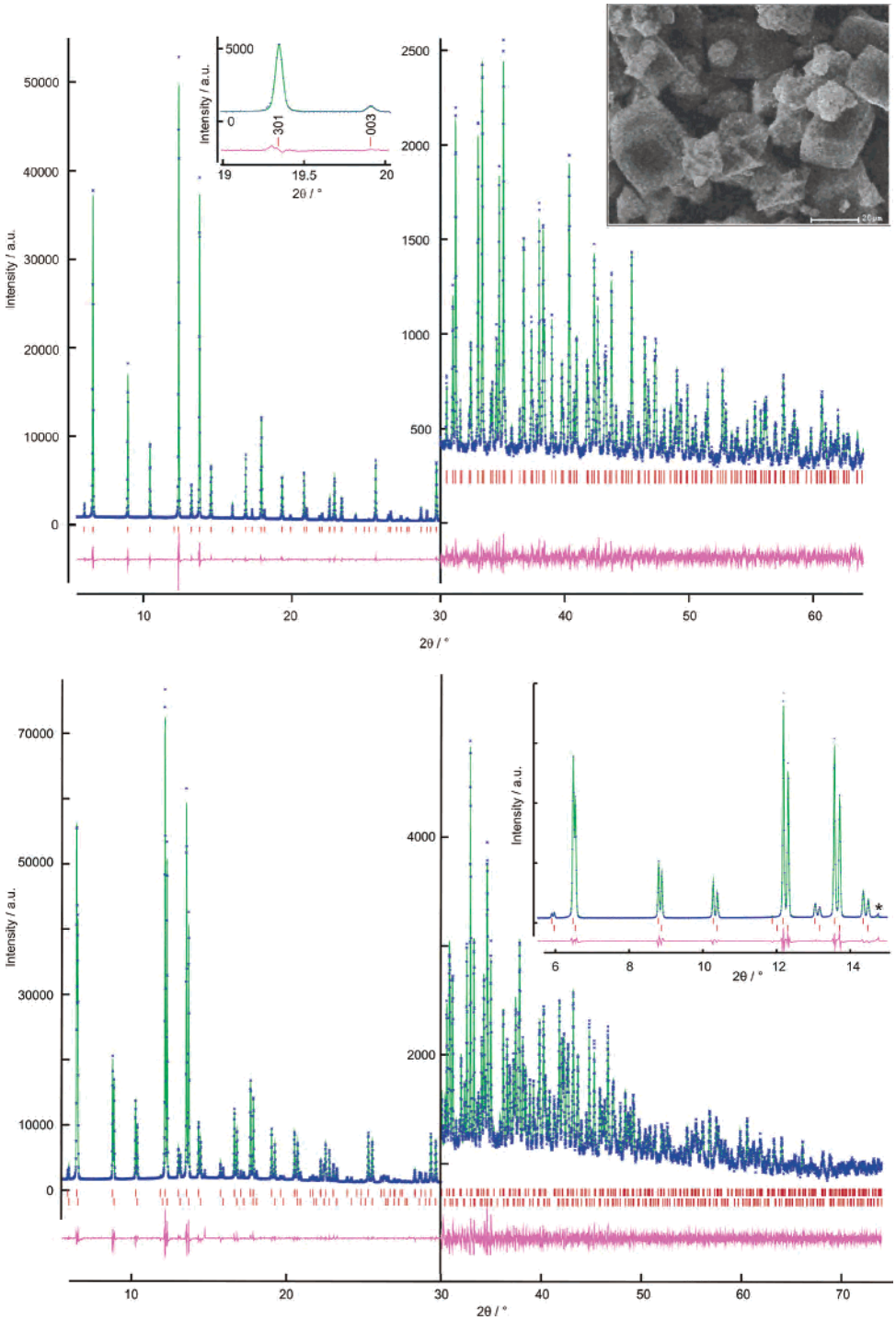

Figure 4. Le Bail fitted synchrotron powder patterns. The high angle parts are drawn at different scales to ensure clearness. The observed and calculated data are marked with crosses and lines, respectively. The Bragg reflection positions are indicated with vertical ticks, and the difference curves are shown at the bottom. Top: $[Fe(4ditz)_3](PF_6)_2$ ethanol solvate at 100 K, $\lambda = 1.001\ 19$ Å. The insets show an expanded section of the pattern, illustrating the anisotropic reflection broadening (left), and a SEM image of the as-precipitated sample (right) ($R_{wp} = 0.049$, $\chi^2 = 1.78$). Bottom: $[Fe(4ditz)_3](PF_6)_2$ methanol solvate at 175 K (heating cycle), $\lambda = 1.0005$ Å. The inset illustrates the splitting of the reflections due to phase segregation. The asterisk marks ice formed on the capillary's surface upon cooling ($R_{wp} = 0.037$, $\chi^2 = 2.48$).

underline the correctness of the refinement (the results of the remaining patterns are of comparable quality). The powder patterns of both solvates are characterized by the absence of amorphous and crystalline impurities and an extraordinarily high degree of crystallinity. The latter is most likely caused by the infinite three-dimensional networking of the iron(II)−tetrazole octahedra providing a rigid framework. The crystallites assume the shape of isometric rhombohedra with an average size of 20 μm (see right inset in Figure 4 top). These properties are reflected in narrow reflections with fwhm's ranging from ≈0.04° to 0.17° (in 2θ), which is comparable to the CeO_2 standard at low angles. This allows the separation of reflections at high angles providing highly reliable lattice parameters. Already visible to the naked eye is the additional anisotropic broadening of the 00l compared to neighboring reflections (see left inset

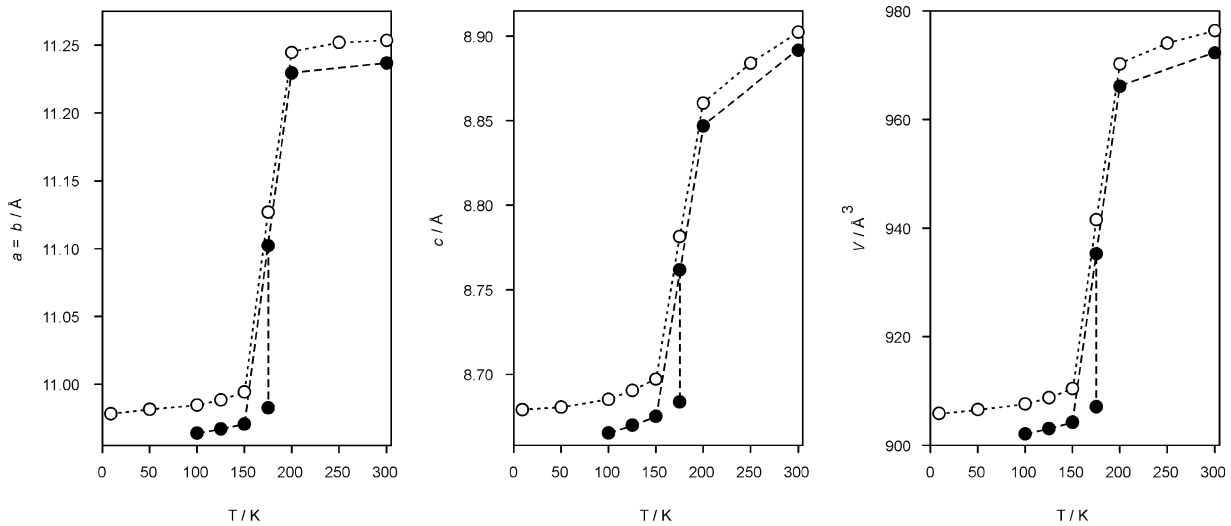

Figure 5. Temperature-dependent lattice parameters and unit-cell volumes of the $[Fe(4ditz)_3](PF_6)_2$·solvates (SG $P\bar{3}$ (No. 147)) during cooling. (● = methanolate, ○ = ethanolate). The error bars are smaller than the representation symbols. The two-phase mixtures that are observed at 175 K for the methanol solvate are discussed in the text.

in Figure 4 top). This observation is confirmed by the profile parameters that clearly indicate a larger variation of the *c*-axis length as compared to the perpendicular crystallographic directions (compare parameter S004 in the Supporting Information, p S10). That can be explained by the disordered and therefore irregular incorporation of MeOH/EtOH molecules that are located on the 3-fold axis: that is, the mostly affected lattice parameter is *c*. No obvious dependence and significant change of the profile shape parameters on temperature cycling were observed. This means that the crystallites are not broken down while switching from the HS to the LS state and reverse. Likewise, no additional microstrain is built up during thermal treatment. The change in the Fe(II)−N bond lengths by about 10% on the HS−LS transition is buffered by reduction of the lattice parameters and a slight reorientation of the flexible butylene-chains.

The temperature-dependent behavior of the lattice parameters is illustrated in Figure 5. One can see immediately that in powder form the ethanolate is slightly larger than the methanolate. The thermal contraction of the HS and LS forms is also clearly visible. Note that in Figure 5 only the data obtained through cooling are presented but the complete data are given in the Supporting Information, p S11. The lattice parameters for both solvates are systematically larger during the heating cycle compared to the cooling cycle, but this could arise from imprecise thermostatting of the sample (even a very small error would cause large discrepancies since there is approximately a 10% volume change over 20 K). This is most strongly pronounced for the ethanol HS phase. The patterns that were recorded in the spin-switching regions of the two phases (175 K) yielded unexpected results. In the case of the methanolate, different two-phase mixtures were obtained depending on whether the temperature was lowered or raised (see Figure 4 bottom). On cooling, the methanolate separates into two phases. Phase 1 consists of 96 mol % with 50% of the Fe(II) in the HS and 50% in the LS state. Phase 2 consists of 4 mol % with 3% HS and 97% LS Fe(II). Each phase is a solid solution with a statistical

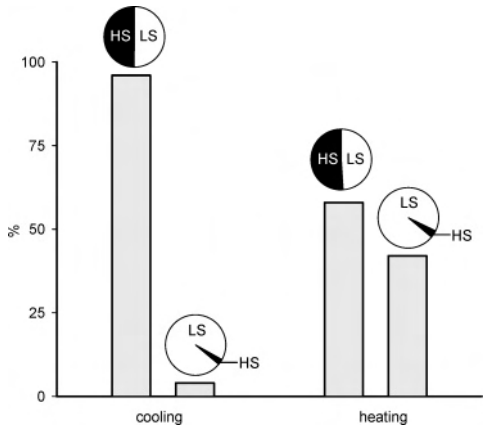

Figure 6. The phase separation observable at 175 K during cooling and heating for $[Fe(4ditz)_3](PF_6)_2$·0.075MeOH. The bar chart shows the percentage of each phase present, and the pie chart describes the HS/LS ratio within each phase.

distribution of the two different iron(II) species on the Wyckoff site 1a. Upon heating, the sample separates again into two different phases: 58 mol % with 51% HS and 49% LS, and 42 mol % with 4% HS and 96% LS. This is shown diagrammatically in Figure 6. The total fractions of the HS and LS states ($T_{cooling}$, 48% HS/52% LS; $T_{heating}$, 32% HS/68% LS) are in very good agreement with the magnetic measurements. For the EtOH solvate, only one pattern around $T_{1/2}$ was measured exhibiting a single phase HS/LS ≈ 1:1 solid solution ($T_{1/2}$ is the temperature at which 50% of the Fe atoms are HS and 50% are LS). To our knowledge this is the first time such a phase segregation of spin-crossover compounds was studied during spin-switching by powder diffraction (apart from Money et al.[22] where such an observation is mentioned for one data set but without further discussion). It has to be pointed out that from the powder diffraction patterns it is impossible to determine where the

(22) Money, V. A.; Evans, I. R.; Elhaïk, J.; Halcrow, M. A.; Howard, J. A. K. *Acta Crystallogr., Sect. B* **2004**, *60*, 41−45.

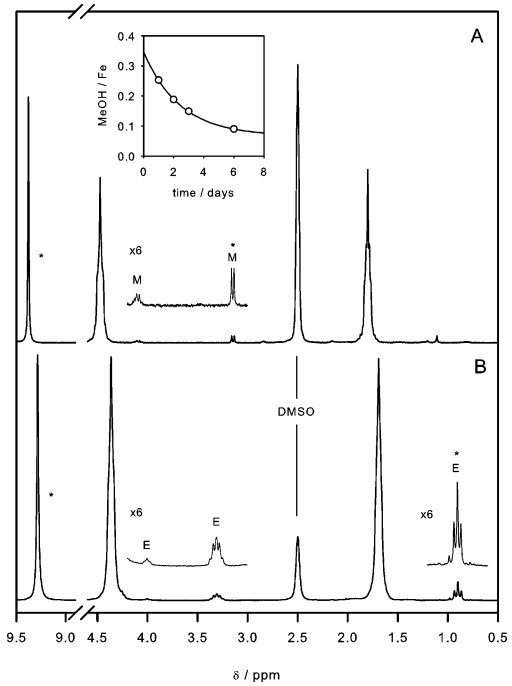

Figure 7. Typical spectra obtained during the ^{1}H NMR determination of the solvent trapped in (A) $[Fe(4ditz)_3](PF_6)_2 \cdot 0.075MeOH$ (6 days after production) and (B) $[Fe(4ditz)_3](PF_6)_2 \cdot 0.25EtOH$. E and M denote the MeOH and EtOH peaks, $*$= peaks used to determine the ratio of CH (tetrazole) to solvent (CH_3). The insert shows the disappearance of MeOH with time. The data have been fitted with a single exponential of the form $A_o \exp(-kt) + \text{const}$. For comparison, the following data for the pure ligand: ^{1}H NMR (200 MHz, DMSO) δ (ppm) 1.76 (4H, m, CH_2), 4.43 (4H, m, CH_2-tz), 9.34 (2H, s, CH(tz)).

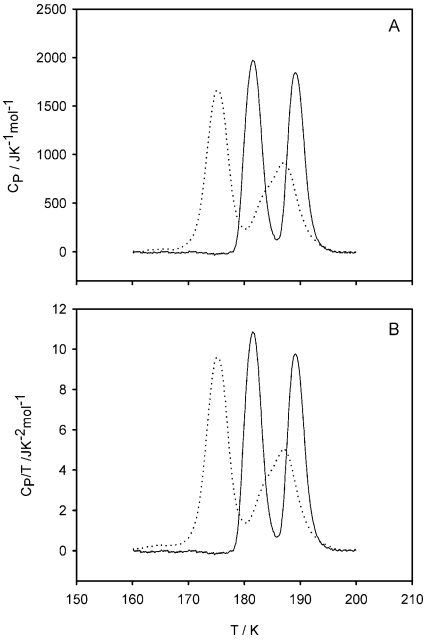

Figure 8. Plots of (A) C_p and (B) C_p/T vs T for $[Fe(4ditz)_3(PF_6)_2] \cdot 0.075MeOH$ (solid line) and $[Fe(4ditz)_3(PF_6)_2] \cdot 0.25EtOH$ (dotted line).

phase separation takes place: It may occur in the crystallites itself, i.e., by forming different domains inside one microcrystal with ascertained LS/HS ratios or by switching entire individuals with constant LS/HS values.

NMR Determination of Solvent. In order to independently determine the solvent present in the powder form, NMR was used. Both coordination polymers dissolve in DMSO-d_6, allowing ^{1}H NMR to be used. To prevent oxidation of iron and to check whether water is not also included, water-free DMSO was used and the NMR tubes were filled in a glovebox under an argon atmosphere. Furthermore, the DMSO alone was measured before addition of the polymers in a glovebox to check how much water the DMSO actually contained. The amount of iron present is very small (5.95% of the total mass of the coordination polymer), and most is present as iron(II), and therefore, although line broadening (approximately 50−100% depending on concentration) and slight concentration dependent peak movement (see Figure 7) are observed, integration was possible and deemed accurate enough for our purposes. The positions of the peaks corresponding to methanol and ethanol were confirmed by adding a drop of methanol and ethanol, respectively. Interestingly, in both cases (see below) splitting ($J = 5.2$ Hz for methanol, $J = 6.9$ Hz for ethanol) is observed between the OH protons and either the CH_3 protons of methanol or the CH_2 protons of ethanol, showing that in DMSO exchange of the OH proton is slow. In the polymer, each iron atom is surrounded by six tetrazole moieties. Therefore, by setting the integral of the CH group of the tetrazole to 6 and then integrating the CH_3 group of methanol or ethanol and dividing this number by 3, we were able to estimate the amount of methanol or ethanol per iron atom (the peaks used are denoted $*$in Figure 7).

Typical spectra are given in Figure 7. The upper spectrum (Figure 7A) shows the methanolate sample dissolved in DMSO 6 days after production, and the lower spectrum (Figure 7B) shows the ethanolate sample: in both cases no water is present. Although the amount of ethanol remains constant at 0.25 ± 0.004 EtOH/Fe, the methanol sample decreases with time (see insert in Figure 7A). The decrease in the amount of MeOH/Fe with days after production of the sample shows clearly an exponential decrease (the data were least-squares fitted to $y = A_o \exp(-kt) + \text{const}$). The experiment was repeated several times with different powder samples and gave a final concentration of 0.075 ± 0.02 MeOH/Fe. It is this final concentration that was used for all physical measurements.

DSC Calorimetry. Calorimetry was used to characterize the compounds and see if changes in the magnetic data could be explained by differing thermodynamic parameters. The heat flow has been converted to a mass heat capacity at constant pressure C_p. C_p and C_p/T have been plotted against T in Figure 8. Numerical integration has yielded ΔH and ΔS, respectively, and the values obtained are given in Table 2. From the plots in Figure 8, one can easily see that the methanolate consists of two sharp peaks referring to the two transitions. The peak temperatures (T_P) do not occur exactly at the transition temperature but are approximately 10 K higher, and this is due to the speed of heating (10 K min^{-1}). The peaks can be integrated separately or together, and the values are given in Table 2. In comparison, the ethanolate shows two peaks that are broader and cannot therefore be separately integrated. Again, the peak temperatures are comparable but lie too high. However, the enthalpy divided

Table 2. Thermodynamic Parameters of the Spin Transition of $[Fe(4ditz)_3](PF_6)_2 \cdot$solv Obtained by DSC Calorimetry

quantity[a]	methanolate	ethanolate
T_{P1}/K	181.5	175.3
T_{P2}/K	189.2	187.0
ΔH/kJ mol^{-1}	13.9	15.3
ΔH_1/kJ mol^{-1}	7.1	
ΔH_2/kJ mol^{-1}	6.8	
ΔS/J K^{-1} mol^{-1}	75.2	89.0
ΔS_1/J K^{-1} mol^{-1}	39.2	
ΔS_2/J K^{-1} mol^{-1}	36.0	
$(\Delta H/\Delta S)$/K	185	172
$(\Delta H_1/\Delta S_1)$/K	181	
$(\Delta H_2/\Delta S_2)$/K	189	

[a] T_{P1} and T_{P2} are the positions of the peak maxima.

by the entropy gives an estimate of the spin transition temperatures, and these are also given and compare favorably with those obtained from SQUID measurements.

Discussion

Although solvent effects in SC compounds have been observed before,[23−25] in all compounds in which the solvent was crystallographically defined, it was hydrogen-bonded to either the iron,[26] the ligand,[27,28] or the anion.[29] In this study, the solvent is trapped within cavities separating iron atoms from different interpenetrating networks. The three tetrazoles forming the face of the octahedra of the iron face the three tetrazoles of the next iron, encapsulating the solvent like two baseball gloves. The solvent is thus far-removed from the anion (approximately 4 Å), and although there may be some interactions with the π electron density of the tetrazoles, there is no conclusive proof of this. Thermogravimetric experiments are inconclusive; the ethanolate sample produces, within experimental error, identical thermogravimetric data compared with the methanolate previously published[8] (see Supporting Information, p S12). The amount of solvent is so low (approximately 1 mass %) that any small decrease in mass before strong exothermic thermal decomposition of the tetrazoles at 250 °C is within the accuracy of the experiment.

Of particular interest is the effect of the inclusion of these solvents on the SC behavior of the compound. As shown above, the structural changes are minimal but lead upon changing to ethanol to a shift of 7 K downward for the transition temperature and disappearance of the hysteresis present in the methanol sample. These differences can almost certainly be explained by the amount and type of solvent present. The single-crystal data show that ideally 0.75 methanol is trapped per iron, compared with 0.25 EtOH/Fe. If the polymers are allowed to precipitate out of solution as a powder rather than form large crystals, then less methanol is trapped and it slowly diffuses out (see NMR results above). The limiting value, presumably determined by the surface to volume ratio, is approximately 0.075 MeOH/Fe. We cannot of course discount the possibility that this methanol is replaced by water as observed in comparable compounds,[30] but interestingly, even though the complex is prepared with $FeCl_2 \cdot 4H_2O$, we observe no water in the NMR experiments. In comparison it seems that the larger ethanol stays and cannot leave the cavity, so regardless whether present as a single crystal or powder, the solvent quantity remains identical and constant. Importantly, all measurements were made using the powder form of both solvates.

Diffusion of the methanol can be explained by the following mechanism: The solvent cannot move directly in the *c* direction due to the iron−tetrazole octahedra and cannot move directly from cavity to cavity, but the solvent can move parallel to the *a*,*b* plane by hopping to small cavities above and below the PF_6 anion (approximately 7 Å^3 at 100 K; see Supporting Information, p S7). At room temperature, the anions rotate and tumble strongly and can act as "revolving doors" as the system is slightly distorted, pushing the solvent further to the next cavity between iron octahedra, which are of course energetically much more favorable. These cavities next to the anions are obviously too small for ethanol to employ.

The DSC data give values for ΔH and ΔS, which are comparable to most other SC compounds.[6,7,9,31,32] It is interesting to note that despite the large difference in concentrations of solvent, the data show similar values of ΔH for both solvates but a difference of 14 J K^{-1} in ΔS. The difference in ΔH of approximately 1 kJ mol^{-1} is near the limit of precision of the DSC method, and indeed the data presented here support the finding that mainly ΔS changes as one changes from one solvent to another. First, Mössbauer spectra of the ethanolate measured at 4.2 and 295 K (see Supporting Information, p S13) are identical to those previously published[8] for the methanolate. This suggests that the direct coordination sphere of the iron is unchanged upon changing from methanol to ethanol. Second, variable temperature far-IR spectra (see Supporting Information, p S14) are also identical for the two solvates.[8] Again, this suggests an unchanged coordination sphere, but it could be that in this case any changes are not observable as they are almost certainly within the accuracy of the experiment. Third, and most importantly, the X-ray data (a combination of single-crystal and synchrotron) show practically no change in the Fe−N distance upon changing from methanol to ethanol. Indeed, there is only a 0.02 Å change in the unit cell parameters *a*, *b*, and *c* in powder form, which corresponds to an approximate 5 Å^3 increase in the unit-cell volume on going from methanol to ethanol (≈0.5%; see Figure 5 and Supporting Information, p S11). Therefore, slight changes in the structure seem to be caused by the need to fit the larger

(23) Takeda, S.; Ueda, T.; Watanabe, A.; Maruta, G. *Polyhedron* **2001**, *20*, 1263−1267.
(24) Sylva, R. N.; Goodwin, H. A. *Aust. J. Chem.* **1968**, *21*, 1081−1084.
(25) Koenig, E.; Ritter, G.; Goodwin, H. A. *Chem. Phys.* **1974**, *5*, 211−223.
(26) Niel, V.; Thompson, A. L.; Munoz, M. C.; Galet, A.; Goeta, A. E.; Real, J. A. *Angew. Chem., Int. Ed.* **2003**, *42*, 3760−3763.
(27) Halder, G. J.; Kepert, C. J.; Moubaraki, B.; Murray, K. S.; Cashion, K. S. *Science (Washington, DC, U.S.)* **2002**, *298*, 1762−1765.
(28) Childs, B. J.; Cadogan, J. M.; Craig, D. C.; Scudder, M. L.; Goodwin, H. A. *Aust. J. Chem.* **1997**, *50*, 129−138.
(29) Guetlich, P. *Struct. Bonding* **1981**, *44*, 83.
(30) Quesada, M.; de Hoog, P.; Gamez, P.; Roubeau, O.; Aromi, G.; Donnadieu, B.; Massera, C.; Lutz, M.; Spek, A. L.; Reedijk, J. *Eur. J. Inorg. Chem.* **2006**, *7*, 1353−1361.
(31) Sorai, M. *J. Chem. Thermodyn.* **2002**, *34*, 1207−1253.
(32) Törnroos, K. W.; Hostettler, M.; Chernyshov, D.; Vangdal, B.; Bürgi, H.-B. *Chem.−Eur. J.* **2006**, *12*, 6207−6215.

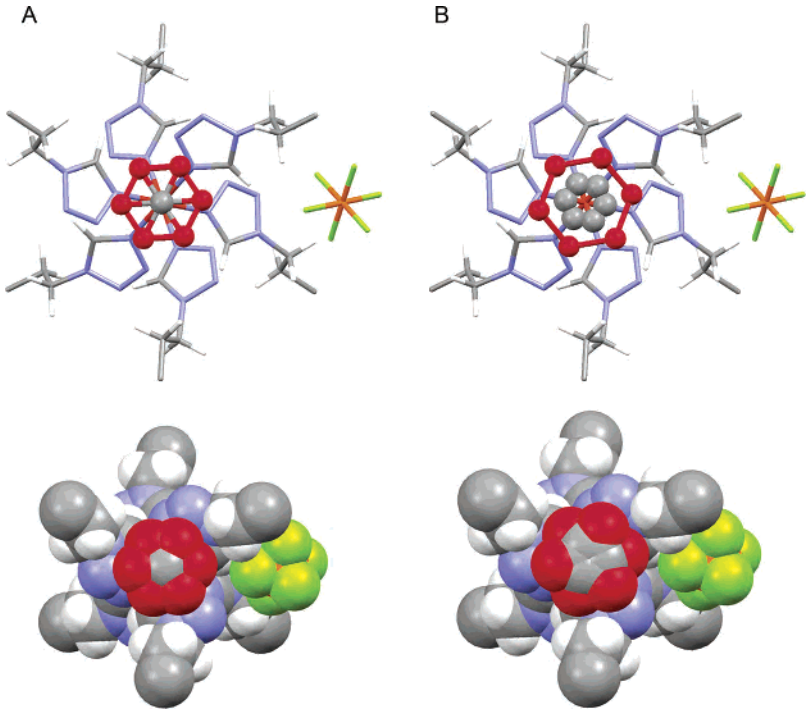

Figure 9. Diagram to illustrate the solvent molecules in all six possible positions in order to show clearly the different rotational properties of (A) methanol and (B) ethanol. Upper figures are capped stick (the red lines do not infer bonds) representations, and the lower are space filling diagrams. In both representations, the gray spheres are carbon atoms, the red spheres are oxygen, the blue spheres are nitrogen, the white spheres are hydrogen, and the yellow spheres are fluorine. All views are down the *c*-axis.

ethanol in and the need for the network to relax by exactly the right amount. The shift in transition temperature observed therefore does not seem to be caused by an increase in "internal pressure",[33,34] even though comparable changes[35−37] in the unit-cell volume caused by the application of an external pressure cause the same shift in $T_{1/2}$ for the extremely well studied $[Fe(phen)_2(NCS)_2]$ polymorph II.

Although the structure consists of three 3D networks, which interpenetrate each other, it can be seen from Figure 1 that the solvent appears between iron atoms of different networks producing effectively parallel 1D "chains" of iron atoms with the solvent statistically distributed in between. However, in contrast to ethanol, methanol is able to move within the polymer, and this might well explain the presence of a hysteresis not observed in the ethanolate.

Conclusions

We report here a detailed study of a triply interpenetrating 3D SC coordination polymer whose magnetic properties can apparently be tuned by inclusion of a different solvent. Such an investigation has been previously completed by Hostettler et al.[11] when studying the family of SC complexes $[Fe(2\text{-}pic)_3]Cl_2\cdot$solv. In contrast to the results presented here, however, the solvent in $[Fe(2\text{-}pic)_3]Cl_2\cdot$solv is hydrogen-bonded to the anion and forms layer-type structures. Furthermore, replacement of the solvent causes large changes in the structure, and therefore one observes greater changes in ΔH than in ΔS during the transition.[31,32] Uniquely we present here a 3D SC metal organic framework, where changes in the caged solvent are accompanied by a very small change in ΔH but significant change in ΔS.

It is interesting to speculate as to the origin of this effect on ΔS. The arrangement of the solvent molecule in a cavity is different for methanol and ethanol. The methanol has a carbon atom at the center, and the oxygen atom is therefore free to adopt any one of the six available positions (the methanol is thus situated almost planar). The ethanol, on the other hand, has a virtual center with one carbon atom on either side and the oxygen atom lying either above or below the plane. There is, therefore, a markedly higher degree of freedom associated with the ethanol system because of the additional CH_2 group, and this will be enhanced if the solvent molecules are free to rotate within their respective cavities. Furthermore, we have shown that in contrast to ethanol, methanol can move within the framework, presumably via small cavities above and below the anion. The above observations are made clear by reference to the spatial arrangements shown in Figure 9.

Finally, we observe a phase separation in the $[Fe(4ditz)_3](PF_6)_2\cdot 0.075$MeOH powder in the plateau of the spin transition at 175 K during cooling and warming. It is not yet clear if this is caused by the switching of different domains or entire crystals. We plan in the future to further

(33) Mueller, E. W.; Ensling, J.; Spiering, H.; Guetlich, P. *Inorg. Chem.* **1983**, *22*, 2074−2078.
(34) Spiering, H.; Kohlhaas, T.; Romstedt, H.; Hauser, A.; Bruns-Ylmaz, C.; Kusz, J.; Guetlich, P. *Coord. Chem. Rev.* **1999**, *190*−*192*, 629−647.
(35) Granier, T.; Gallois, B.; Gaultier, J.; Real, J. A.; Zarembowitch, J. *Inorg. Chem.* **1993**, *32*, 5305−5312.
(36) Guetlich, P.; Ksenofontov, V.; Gaspar, A. B. *Coord. Chem. Rev.* **2005**, *249*, 1811−1829.
(37) Ksenofontov, V.; Gaspar, A. B.; Guetlich, P. In *Spin Crossover in Transition Metal Compounds III*; Gütlich, P., Godwin, H. A., Eds.; Springer: Berlin, 2004; pp 23−64.

investigate this phenomenon and, in addition, to change the anion and observe how this also affects the spin transition.

Acknowledgment. The authors thank Dr. K. Osaka for his help during the powder diffraction experiments at SPring-8. The synchrotron radiation experiments were performed at the beam-line BL02B2 in SPring-8 with the approval of the Japan Synchrotron Radiation Research Insitute (JASRI). We also wish to thank Prof. G. Wiesinger (TU Wien) for Mössbauer measurements, Dipl. Ing. C. Feldgitscher (TU Wien) for thermogravimetric experiments, Prof. P. Simon (STU Bratislava) for use of the DSC, Mrs. K. Poppenberger (TU Wien) and Mr. Y. Hasegawa (Aoyama Gakuin University) for SEM measurements, and Prof. A. Kudryatsev (Mendeleev University Moscow) for useful discussions. M.B. wishes to thank Aoyama-Gakuin University for a 6 week stay and the Marie Curie Training site LAMM (Grant MOLMAG-MEST-CT-2004-504204). G.N.L.J. wishes to thank the Japan Society for the Promotion of Science (JSPS) for funding a 1 month stay in Japan. We wish to thank the following organizations for financial support: Austrian Science Foundation FWF (Project Numbers 15874-N03 and 19335-N17), the Slovakian grant agencies APVV and VEGA, and the Italian MIUR, FIRB (Project RBNE033KMA) and EC for NE "MAGMAnet" (Project NMP3-CT-2005-515767).

Supporting Information Available: Crystal structures as a CIF file, mid-FTIR, SQUID, X-ray single-crystal diffraction studies, synchrotron powder diffraction, thermogravimetry, Mössbauer spectroscopy, and far FTIR spectroscopy. This material is available free of charge via the Internet at http://pubs.acs.org.

IC070173Q